Variations of surface water extent and water storage in large river basins: A comparison of different global data sources

Fabrice Papa, Andreas Güntner, Frédéric Frappart, Catherine Prigent,
William B. Rossow

HAL Id: hal-00442263

https://hal.archives-ouvertes.fr/hal-00442263

Submitted on 18 Dec 2009

Variations of surface water extent and water storage in large river basins: A comparison of different global data sources

F. Papa

NOAA-CREST, City College of New York,
New York, USA

A. Güntner

GeoForschungsZentrum,
Potsdam, Germany

F. Frappart

CESBIO,
Toulouse, France

C. Prigent

LERMA, CNRS, Observatoire de Paris,
Paris, France

W. B. Rossow

NOAA-CREST, City College of New York,
New York, USA

Abstract

For the period 2003–2004 and for six large river basins, the present study compares monthly time series of multi-satellite-derived surface water extent with other independent global data sets related to land water dynamics, such as water mass variations monitored by GRACE, simulated surface and total water storage from WGHM, water levels from altimetry, and GPCP precipitation estimates. In general, the datasets show a strong agreement with each other at seasonal timescale. In particular, over the Amazon and the Ganges basins, analysis of seasonal phase differences and hysteresis behavior between surface water extent, water level and storage reveal the complex relations between water extent and storage variations and the different effects of water transport processes within large river basins. The results highlight the value of combining multi-satellite techniques for retrieving surface water storage dynamics.

1. Introduction

Terrestrial water is critical to sustaining life on Earth and plays a primary role in the global water cycle and climate. Among the different reservoirs in which terrestrial water is stored, surface waters comprised of rivers, lakes, man-made reservoirs, wetlands, and episodically inundated areas are of particular importance because they interact more directly with the ocean and atmosphere through vertical and horizontal mass fluxes. In particular, analysis of

1

variations in surface fresh water extent and storage is a key to understanding the hydrological processes and the global water cycle.

However, with approximately 60% of the world river floodplains and wetlands inundated only during some portion of the year [Matthews, 2000], seasonal and interannual variations in continental surface-stored water volumes at regional-to-global scales, as well as their impact on precipitation, evaporation, infiltration, and runoff, are still not well-known [Bullock and Acreman, 2003]. Lacking spatially complete measurements of inundation/wetland locations, sizes, and water volume changes, it is difficult to verify how hydrologic models properly partition precipitation among these several components and represent their effects on river discharge at continental-to-global scales [Coe et al., 2002; Alsdorf et al., 2007a]. Consequently, the need for better long-term observations of land water extent and storage variations over the whole globe is now recognized [Alsdorf et al., 2007a].

Remote sensing techniques have been very useful to hydrology investigations over the last fifteen years [Alsdorf et al., 2007a; Alsdorf and Lettenmaier, 2003]. For example, satellite altimetry has been used for systematic monitoring of water levels of large rivers, lakes, and floodplains [Birkett, 1998]. Interferometric synthetic aperture radars (SARs) have long been shown capabilities to study flood dynamics and their complexity, especially in the Amazon basin [Alsdorf and Lettenmaier, 2003; Alsdorf et al., 2007b]. Since 2002, the GRACE gravity mission offers, for the first time, direct estimates of the spatio-temporal variations of total terrestrial water storage (the sum of ground water, soil water, surface water, and snow pack) [Ramillien et al., 2005; Schmidt et al., 2006] from month to several year timescales. However at this time, direct estimates of surface water volume and their dynamics at continental/global scales are not available and rely mainly on simulations from hydrological models.

F. Frappart et al. (Interannual variations of river water storage from a multiple satellite approach: A case study for the Rio Negro River basin, submitted to Journal of Geophysical Research, 2007) proposed a new technique to derive spatio-temporal variations of surface water volume over the Negro River basin, the tributary which carries the largest discharge volume to the Amazon River. The method is based on the combination of multi-satellite-derived surface water extent estimates (~25 km sampling intervals) [Prigent et al., 2007; Papa et al., 2006] and water levels over rivers and floodplains from both Topex/Poseidon (T/P) altimeter and in situ hydrographic stations. Monthly surface water volume changes were produced with a maximum error of 23 % over eight successive years (1993–2000), the period of common availability of T/P and the multi-satellite data at this time. The estimates show excellent agreement in the seasonal cycle with GRACE-derived total water mass variations.

The global dataset that quantifies the monthly distribution of surface water extent has been extended to a 12-year record (1993–2004) (F. Papa et al., Interannual variability of surface water extent at global scale, 1993–2004, submitted to Journal of Geophysical Research, 2008) and now overlaps the GRACE measurements for two entire years 2003–2004. The objective of the present study is to compare the surface water extent dataset with other different and independent related land water components and their variations at the scale of large river basins (Amazon, Ganges, Congo, Mekong, Mississippi, Niger). These variables include surface and total water storage derived from satellite (GRACE) and modelling (WGHM), precipitation estimates (GPCP), T/P altimeter-derived inland water-body level heights and in situ river discharge. These comparisons will help better illustrate the complex relations between surface water extent and storage at the scale of large river basins and highlight the

value of using multi-method and multi-satellite techniques to retrieve surface water storage dynamics and improve our understanding of the terrestrial water cycle.

2. Data Sets

In this study, the analysis includes:

1) A dataset that quantifies at global scale the monthly distribution of surface water extent (SWE) and its variations at ~25 km sampling intervals. The methodology which captures the extent (with an accuracy of ~10%) of episodic and seasonal inundations, wetlands, rivers, lakes, and irrigated agriculture over more than a decade, 1993–2004, is based on a clustering analysis of a suite of complementary satellites observations, including passive (SSM/I) and active (ERS) microwaves, visible and near-IR (AVHRR) observations [Prigent et al., 2007; Papa et al., 2006, submitted manuscript, 2008].

2) The GRACE-derived land water mass solution. The GRACE mission, launched on the 17th of March 2002, is devoted to measuring spatio-temporal changes in Earth's gravity field. Several recent studies have shown that GRACE data over the continents provide important information on the total land water storage [Schmidt et al., 2006; Ramillien et al., 2005] with an accuracy of ~1.5 cm of water thickness equivalent when averaged over a few hundred kilometers. Here we use the three latest land water solutions (RL04) provided by GFZ, JPL (for these two first products, January 2003, June 2003 and January 2004 are missing), and CSR (June 2003 and January 2004 are missing) with a spatial resolution of ~400 km and processed as in work by Chambers [2006]. These three datasets are available at http://gracetellus.jpl.nasa.gov/.

3) Surface and total water storage from the WaterGAP Global Hydrology Model (WGHM). WGHM represents the continental water cycle at 0.5° spatial intervals [Döll et al., 2003] and has been widely used to analyze spatio-temporal variations of water storage components globally and for large river basins [Güntner et al., 2007]. Here, we use the latest WGHM simulations [Hunger and Döll, 2007] forced with precipitation from the Global Precipitation Climatology Centre (GPCC) [Rudolf and Schneider, 2005] and air temperature, radiation, and number of rain-days within each month from ECWMF operational forecasts.

4) Precipitation estimates from the Global Precipitation Climatology Project (GPCP) that quantify the distribution of precipitation over the global land surface [Adler et al., 2003]. We use the Satellite-Gauge Combined Precipitation Data product Version 2 data, whose estimates uncertainties over land range between 10%–30%. Note that the GPCC data used to force WGHM are the in situ component of GPCP.

5) Topex/Poseidon (T/P) radar altimeter-derived water level heights over large water bodies. First devoted to ocean studies, T/P is commonly used to monitor water levels over lakes, rivers and floodplains [Birkett, 1998] and provide time series of river/inundation level variations from 1993 to mid-2002, before its orbit was changed. In this study, we use the data from the HydroWeb database [Gennero et al., 2005] (available at http://www.legos.obs-mip.fr/en/soa/hydrologie/hydroweb/). For the selected points here, the uncertainty associated with the water level height over the Amazon and the Ganges basins ranges between 10–30 cm for high water season to 30–80 cm during low water season.

3. Results and Discussion

Figure 1 compares the monthly time series of precipitation, SWE and the surface and total water storage over 2003–2004 for six large river basins (the data are aggregated to basin averages), representing different environments from tropical, mid-latitudes, and semi-arid regions. For each time series, the 2-year mean is removed and the resulting anomalies are normalized by their standard deviations. Table 1 summarizes the maximum linear correlation coefficients of point time records between the SWE and the other variables when lagged in time (months). In view of the short time span considered here, the signal is dominated by seasonal variations. Regardless of the environment, Figure 1 and Table 1 show that the seasonal patterns of the time series are similar and show highly significant correlations.

For the Amazon basin, the time records in Figure 1a and Table 1 show that the annual variations of precipitation lead the variations of the surface water extent by 2 months (R = 0.84 with a lag of 2 months). This time lag illustrates that stream flows in upstream regions contribute with a delay in time to large downstream flooding due to the long concentration times in the large hydrographic network of the Amazon. The seasonal variation of SWE is in phase with the surface and total water storage variations (R > 0.89). This implies that inundation area may be a good indicator of actual surface water volumes in this basin and supports earlier studies showing that mass variations in surface water bodies in the Amazon basin contribute significantly to the total storage variations [Matsuyama and Masuda, 1997; Güntner et al., 2007]. Too large large-scale water transport velocities in the model may explain that the simulated surface water storage leads the annual cycle of the other variables by 1 month.

For the Ganges basin (Figure 1b), which receives intense local rainfall during the annual monsoon, the precipitation and the SWE are highly correlated with no lag in time (R = 0.93). SWE variations lead variations in volume storage from GRACE and WGHM by one month with R > 0.79. As for the Ganges, SWE of the Mekong (Figure 1d) and the Niger (Figure 1f) basins are also controlled by large precipitation events during the rainy season with a delay of 1 month relative to the rainfall variations. For both basins, the storage variables follow closely the seasonality of SWE also with a delay of 1 month (R > 0.89), except for the simulated surface water storage.

The Congo and the Mississippi basins, Figures 1c and 1e, exhibit less agreement between the different variables, especially regarding the amplitude of the signal. The Congo SWE shows a fair correlation with the precipitation and GRACE variations but a poor agreement with the simulated surface water storage from WGHM. The disagreement of total water storage between WGHM and GRACE over the Congo reveals the difficulty of hydrological models to properly represent the complexity of the entire Congo basin. Congo sub-basins have different responses to rainfall in terms of flood and storage dynamics due to different soil properties across the basin [Laraque et al., 2001]. In addition, during periods of high anomaly in precipitation (for instance early 2003 and end 2004), 60–70% of rainfall is lost by runoff and evapotranspiration [Crowley et al., 2006]. For the Mississippi, the SWE estimates show a lower correlation with GRACE and poor agreement with the precipitation estimates and the simulated volume storage. These generally lower correlations show that surface water storage is a minor contribution to total storage in the Mississippi watershed [Lettenmaier and Famiglietti, 2006] and that the basin hydrology is complicated by the flood dynamics partially driven by spring snowmelt in the upper portions of the basin.

Phase differences between precipitation, water surface extent, and water storage observed in Figure 1 and in the lagged temporal correlations in Table 1 reveal the different effect of water transport processes within large river basins. A delay of the seasonal cycle of water extent relative to precipitation (Amazon, Mekong, Niger) indicates the large water travel and accumulation times in large river basins that may lead to inundation at downstream locations of the basin even if the basin-average rainfall maximum has been passed. Focusing on the Amazon and the Ganges basins, Figure 2 illustrates two different cases of the complex dynamics between the variations in the SWE and the variations in the surface and total water storage. Figure 2 compares the mean seasonal cycle 2003–2004 (for available months) between the SWE and the total water storage from GRACE CSR (Figures 2a and 2d) and between the SWE and the simulated surface water storage from WGHM (Figures 2b and 2e). We also compare here the normalized mean seasonal cycle calculated over 1993–2000 between the SWE and the altimeter level height from T/P for some locations across the two basins (Figure 2c for the Amazon and Figure 2f for the Ganges). Frappart et al. (submitted manuscript, 2007) demonstrated that surface water volume change can be derived from the multi-satellite SWE combined with T/P water level heights. Over the Amazon, we also display the mean seasonal cycle 1993–2000 for the in situ river discharge at Obidos (2.50 S; 55.51 W) a location close to the altimeter level measurements (at 2.50 S; 56.50 W).

Figure 2 clearly shows that the two basins exhibit different regimes with different hydrological phases. For the Amazon, Figures 2a and 2b show that the mean annual cycle can be divided into sub-periods where the SWE and the volume storage varying together: a low water period from September to November, a rising period from January to April, a high water period in April–May and a falling period from June to September. The surface storage and the total storage show differences with a quicker decrease of surface storage during the period of decreasing inundation area. This suggests a longer residence time of soil water and groundwater as part of total storage, but may also point to model deficiencies, i.e., too rapid surface water transport. In addition, Figure 2c clearly shows that the mean annual cycles between the SWE, the water level height, and the discharge have patterns close to the ones observed between the SWE and the volume storages. In the case of the Amazon, SWE and water stage increase/decrease roughly simultaneously, leading to an approximately unique relationship between water extent/level and volume for aggregated basin-scale values.

The Ganges basin shows a totally different regime than the Amazon basin, with a strong hysteresis behavior between the SWE and the storage components (Figures 2d and 2e). The minimum period is from January to May and the rising period shows a large increase of both SWE and water storage as the monsoon season starts. With the SWE at maximum in July, surface and total water volume are still increasing in August. The falling period, from September to December, shows a sharp decrease in SWE while water storage remains high and decreases more slowly. Figure 2f shows a similar behavior between the SWE and the water level heights and confirms a strong hysteresis pattern, especially for downstream locations in the river basin (black and red). In these cases, due to large water transport times through the river network, high water levels occur comparatively late in the monsoon season when inundation in the upstream parts of the basin are at the maximum or starting to decline. The hysteresis between water extent and storage indicates widespread shallow flooding in the river basin with the onset of the monsoon period, including flooding of irrigated agricultural areas (e.g. paddy fields). These shallow inundation areas rapidly dry out after the end of the rainy season (see the high correlation without time lag between precipitation and water extent in Table 1), while large water masses remain stored in the main floodplains and the delta

regions which continue to receive water from the entire watershed and additional precipitation.

4. Conclusion

This study reports a first effort to compare and analyze the variations of multi-satellite-derived surface water extent with precipitation estimates, water mass variations monitored by GRACE and surface and total water storage simulated by WGHM. Over six major river basins and for a 2-year period (2003–2004), the different data sets show in general good agreement in their seasonal variations. Over the Amazon and the Ganges, analysis of phase differences and hysteresis behavior in the mean annual cycle between surface water extent, water level height and water storage demonstrate the complex relations between these variables at the scale of large river basin. The delay with which an increase in inundation extent translates into a major increase of surface water volumes depends on the water transport processes and flow concentration times of the river basin.

The results highlight that a combination of the surface water extent dataset and altimeter-derived water level height in order to derive surface water volume change, as proposed by Frappart et al. (submitted manuscript, 2007) over the Negro Rio, could be successfully applied to other large river basins. In combination with near-future soil moisture products derived from SMOS, it will allow for the first time a decomposition of the total water storage monitored by GRACE into its several components.

References

Adler, R. F., et al. (2003), The version 2 Global Precipitation Climatology Project (GPCP) monthly precipitation analysis 1979–present, J. Hydrometeor., 4, 1147–1167.

Alsdorf, D. E., and D. P. Lettenmaier (2003), Tracking fresh water from space, Science, 301, 1492–1494.

Alsdorf, D. E., E. Rodríguez, and D. P. Lettenmaier (2007a), Measuring surface water from space, Rev. Geophys., 45, RG2002, doi:10.1029/2006RG000197.

Alsdorf, D., P. Bates, J. Melack, M. Wilson, and T. Dunne (2007b), Spatial and temporal complexity of the Amazon flood measured from space, Geophys. Res. Lett., 34, L08402, doi:10.1029/2007GL029447.

Birkett, C. M. (1998), Contribution of the TOPEX NASA radar altimeter to the global monitoring of large rivers and wetlands, Water Resour. Res., 34(5), 1223–1239.

Bullock, A., and M. C. Acreman (2003), The role of wetlands in the hydrological cycle, Hydrol. Earth Syst. Sci., 7(3), 75–86.

Chambers, D. P. (2006), Evaluation of new GRACE time-variable gravity data over the ocean, Geophys. Res. Lett., 33, L17603, doi:10.1029/2006GL027296.

Coe, M. T., M. H. Costa, A. Botta, and C. Birkett (2002), Long-term simulations of discharge and floods in the Amazon Basin, J. Geophys. Res., 107(D20), 8044, doi:10.1029/2001JD000740.

Crowley, J. W., J. X. Mitrovica, R. C. Bailey, M. E. Tamisiea, and J. L. Davis (2006), Land water storage within the Congo Basin inferred from GRACE satellite gravity data, Geophys. Res. Lett., 33, L19402, doi:10.1029/2006GL027070.

Döll, P., F. Kaspar, and B. Lehner (2003), A global hydrological model for deriving water availability indicators: Model tuning and validation, J. Hydrol., 270, 105–134.

Gennero, M. C., J. F. Cretaux, M. B. Nguyen, C. Maheu, K. Do Minh, S. Calmant, and A. Cazenave (2005), HydroWeb, Surface water monitoring by satellite altimetry, Lab. d'Etudes en Geod. et Oceanogr. Spatiale, Toulouse, France.

Güntner, A., J. Stuck, S. Werth, P. Döll, K. Verzano, and B. Merz (2007), A global analysis of temporal and spatial variations in continental water storage, Water Resour. Res., 43, W05416, doi:10.1029/2006WR005247.

Hunger, M., and P. Döll (2007), Value of river discharge data for global-sale hydrological modeling, Hydrol. Earth Syst. Sci. Discuss., 4, 4125–4173.

Laraque, A., G. Mahe, D. Orange, and B. Marieu (2001), Spatiotemporal variations in hydrological regimes within central Africa during the XXth century, J. Hydrol., 25, doi:10.1016/S0022-1694(01)00340-7.

Lettenmaier, D. P., and J. S. Famiglietti (2006), Hydrology: Water from on high, Nature, 444, 562–563.

Matsuyama, H., and K. Masuda (1997), Estimates of continental-scale soil wetness and comparison with the soil moisture data of Mintz and Serafini, Clim. Dyn., 13(10), 681–689.

Matthews, E. (2000), Wetlands in Atmospheric Methane: Its Role in the Global Environment, edited by M. A. K. Khalil, pp. 202–233, Springer, New York.

Papa, F., C. Prigent, F. Durand, and W. B. Rossow (2006), Wetland dynamics using a suite of satellite observations: A case study of application and evaluation for the Indian Subcontinent, Geophys. Res. Lett., 33, L08401, doi:10.1029/2006GL025767.

Prigent, C., F. Papa, F. Aires, W. B. Rossow, and E. Matthews (2007), Global inundation dynamics inferred from multiple satellite observations, 1993–2000, J. Geophys. Res., 112, D12107, doi:10.1029/2006JD007847.

Ramillien, G., F. Frappart, A. Cazenave, and A. Güntner (2005), Time variations of the land water storage from an inversion of 2 years of GRACE geoids, Earth Planet. Sci. Lett., 235, 283–301.

Rudolf, B., and U. Schneider (2005), Calculation of gridded precipitation data for the global land-surface using in-situ gauge observations, in Proceedings of the 2nd Workshop of the International Precipitation Working Group IPWG, Monterey, October 2004, pp. 231–247, Eur. Organ. for the Exploit. of Meteorol. Satell., Darmstadt, Germany.

Schmidt, R., et al. (2006), GRACE observations of changes in continental water storage, Global Planet. Change, 50, 112–126.

TABLES

Table 1. Maximum Time-Lagged Linear Correlation Coefficient Between the Surface Water Extent and the Precipitation, the Total Water Storage From GRACE and the Simulated Water Storage From WGHM for the Six Basins[a].

	GPCP Precipitation (mm/month)	Total Water Storage (km³)			WGHM Water Storage (km³)	
		GFZ	JPL	CSR	Surface	Total
Amazon	0.84 (−2)	0.95	0.95	0.95	0.93 (−1)	0.89
Ganges	0.93	0.79 (+1)	0.79 (+1)	0.79 (+1)	0.84 (+1)	0.84 (+1)
Congo	0.71	0.83	0.83	0.85	0.69 (+1)	0.61
Mekong	0.89 (−1)	0.89 (+1)	0.89 (+1)	0.89 (+1)	0.94	0.94 (+1)
Mississippi	0.48 (+1)	0.69	0.69	0.69	0.51	0.61 (−2)
Niger	0.90 (−1)	0.86 (+1)	0.86 (+1)	0.84 (+1)	0.81 (+1)	0.94

[a]Surface water extent is in km². Time lag in month to obtain the maximum correlation is in parentheses. For instance over the Amazon, the surface water extent and the precipitation have a maximum correlation of 0.84 with the precipitation preceding the surface water extent with 2 months. For the comparison with the precipitation and the model (24 months), p-values < 0.01 for R > 0.51, with GRACE-CSR (22 months), p-values < 0.01 for R > 0.53 and with GRACE-JPL and GFZ (21 months), p-values < 0.01 for R > 0.55.
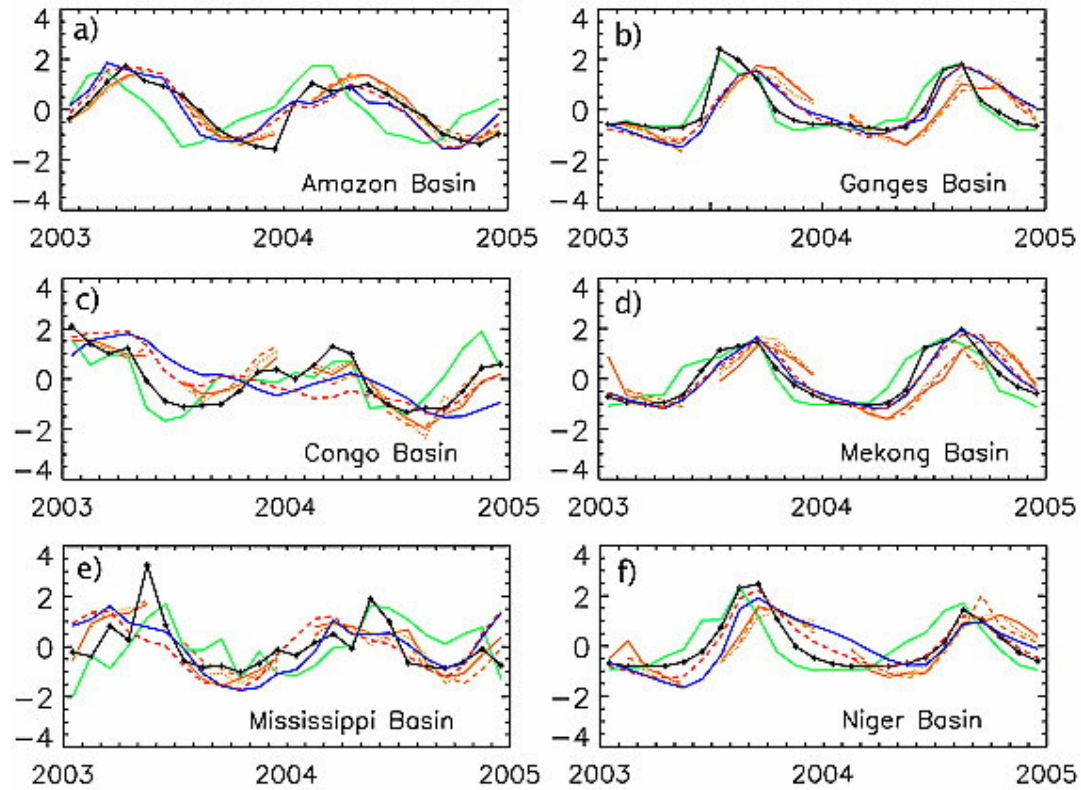
FIGURES

Figure 1. Time series of satellite-derived inundation extent (black), GRACE-derived total water storage (yellow; version 4 from CSR solid line; version 4 from GFZ dotted line, version 4 from JPL dashed line), WGHM simulated total water storage (dashed red), WGHM simulated surface water storage (blue) and GPCP precipitation (green) for six large river basins during the 2003–2004 period. All variables are normalized (the mean is subtracted and the resulting values are divided by the standard deviation over the period).
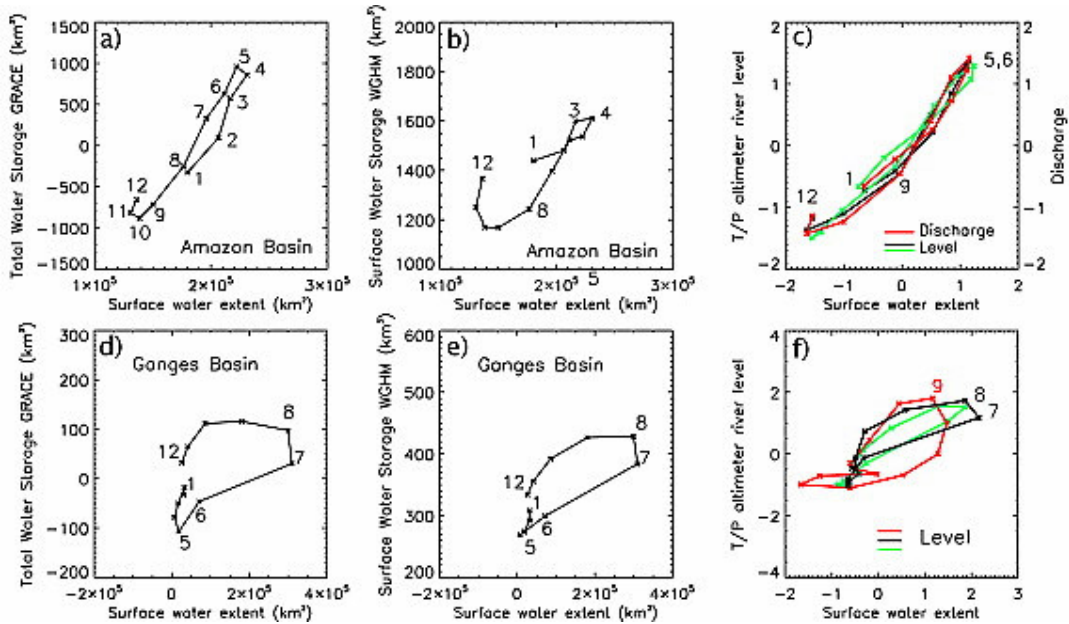
9

Figure 2. (a, d) Mean seasonal cycle between the satellite-derived surface water extent and GRACE-derived total water storage version 4 from CSR for the Amazon and the Ganges basins during the 2003–2004 period (the numbers represent the month of the year). (b, e) 2003–2004 mean seasonal cycle between the multi-satellite-derived surface water extent and WGHM simulated surface water storage. (c) Mean seasonal cycle (normalized anomaly) between the satellite-derived surface water extent and altimeter-derived river level heights (black for (2.50 S; 56.50 W), green for (−3.23 S; 59.50 W)) and between the in situ river discharge at Obidos (red (2.50 S; 55.51 W)) for the Amazon. (f) Mean seasonal cycle (normalized anomaly) between the satellite-derived surface water extent and altimeter-derived river level height for the Ganges (black for (27.93 N; 78.86 E), green for (25.50 N; 85.70 E), red for (23.27 N; 89.55 E)). (c and f) The mean cycles are calculated over the period 1993–2000 and the surface water extent is calculated on a 2° × 2° area centered on the altimeter water level estimates.